Vol. 2 No. 4 (2024)

Spectrum of Engineering Sciences

SPECTRUM OF ENGINEERING SCIENCES

Online ISSN
3007-3138
Print ISSN
3007-312X

Retrofitting Strategies for Enhancing Wind Resilience of Minor Structures: A Numerical Investigation

Saad Zaheer[1]
Centre of Excellence in Water Resources Engineering, University of Engineering and Technology (UET), Lahore, Pakistan,
Civil Engineering Department, Bahauddin Zakariya University, Multan, Pakistan
saad.ahmad4456@gmail.com

Naheed Akhtar[2]
Abasyn University, Islamabad, Pakistan
naheed.akhtar@abasynisb.edu.pk

Sardar Junaid Asad[3]
Capital University of Science and Technology, Islamabad, Pakistan
sardarjunaidasad@gmail.com

Mehran Khalil[4]
Site Inspector, National Highway Authority (NHA), Balochistan, Pakistan
mehrankhalil0@gmail.com

Tahir Sultan[5]
Civil Engineering Department, Bahauddin Zakariya University, Multan, Pakistan
tahirsultan@bzu.edu.pk

Dr. M. Adil Khan[6]
Resident Engineer (RE), National Engineering Services Pakistan (NESPAK), Lahore, Pakistan
adee.uol@gmail.com

Abstract

The collapse of a tensile fabric parking shelter with an arched roof under severe wind loads is numerically analyzed in this study. Under simulated wind

Vol. 2 No. 4 (2024)
Spectrum of Engineering Sciences
Online ISSN
3007-3138
Print ISSN
3007-312X

conditions, the project assesses the structural reactions and pinpoints the crucial failure sites using LS-DYNA's sophisticated finite element analysis capabilities. To create an accurate simulation model, the inquiry starts with a thorough site inspection, during which material samples and structural dimensions are gathered. The work effectively compares a comprehensive finite element model to the actual failure using LS-DYNA, which captures the intricate behaviors of the structural components under wind loads. Using this analysis, we pinpoint essential design flaws in the parking structure and suggest two repair plans to strengthen structural resistance against comparable wind-driven collapses. Additionally, the project creatively compares uplift on several canopy designs using wind tunnel testing, recommending the best design to reduce wind-induced damages. By improving our knowledge of wind dynamics and structural reaction, the investigation's conclusions not only shed light on the parking shed's particular collapse process but also advance the civil engineering discipline.

Keywords: LS-DYNA, Arched Roof, material model validation, benchmarking, retrofits, uplift, wind tunnel

Introduction

Because the transportation system developed so quickly in the late 19th and early 20th centuries, riveted steel construction became increasingly prevalent. The frequency of loads and the consequences of fatigue on these structures grew with further innovations and reliance on transportation [1-2]. These riveted constructions are nearing the end of their design life, which is 100 years, and are consequently increasingly vulnerable to fatigue-based failure. Kuhn et al. [3] noted how common it is to reinforce and repair these structures to prolong their design life and avoid fatigue failure. Until the middle of the 20th century, when prefabricated steel structures like welded and hot-rolled sections took over as the most common product for usage in the steel building sector, riveted steel structures remained popular.

Engineers and designers favor prefabricated steel buildings above other steel products, even today. Although these steel buildings have not existed long enough to reach the 100-year design life, fatigue-based damage is developing in these structures [4]. Older bridges are exposed to higher loading circumstances than the original design loads because of technical breakthroughs and advances in engineering expertise. Compared to when

Spectrum of Engineering Sciences
SPECTRUM OF ENGINEERING SCIENCES
Online ISSN
3007-3138
Print ISSN
3007-312X

they were first built, steel bridges are now subjected to greater amplitude and frequency loadings [5]. Due to their extensive use in public and private infrastructure, tensile steel fabric structures' robustness and durability, especially in harsh weather conditions, have emerged as a key area of study in modern civil engineering [6]. Although progressive collapse, which may be caused by impact, blast, or fire, is another dangerous consequence of inadequate robustness design, low-cycle fatigue (LCF) failure has been identified as one of the most frequent failure modes of structures that experience a significant earthquake. Solving both problems with a consistent design approach might be difficult because of the different performance needs [7]. Despite their aesthetic appeal and practical versatility, these lightweight constructions are vulnerable to dynamic environmental factors, particularly wind [8].

The mechanical properties of cold-formed steels differ significantly from those of virgin steel sheets before forming, and hot-rolled steels are attributable to the cold-forming process. The yield and tensile strength increase while ductility decreases during these processes. The deformations occurring during the fabrication process in flat regions tend to be elastic, while those at the corners are predominantly plastic. Three phenomena contribute to the changes in mechanical properties during cold forming: strain hardening, strain aging, and the Bauschinger effect, which indicates that the longitudinal compression yield strength of stretched steels is lower than the longitudinal tension yield strength. The additional cold-forming strength diminishes with increasing temperature and is lost above 500 °C.

The existing design codes, including BS 5950 Part 8 [9] and EN 1993-1-2:2005 [10], offer reduction factors for the mechanical properties of cold-formed steels at elevated temperatures, albeit with certain limitations. The BS 5950 Part 8 [9] specifies reduction factors for yield strengths at 0.5%, 1.5%, and 2.0% strain levels, while EN 1993-1-2:2005 [10] offers identical reduction factors applicable to class 4 hot-rolled steels.

According to Sidey and Teague [11], the strength reduction of cold-formed steels at elevated temperatures can be 10–20% greater than that of hot-rolled steels, attributed to differences in metallurgical composition and molecular surface effects [12-13]. Several studies have examined the mechanical properties of cold-formed steels at elevated temperatures,

Spectrum of Engineering Sciences
SPECTRUM OF ENGINEERING SCIENCES
Online ISSN
3007-3138
Print ISSN
3007-312X

focusing on low and high-strength variants across various thicknesses. Most of these studies indicate that the yield strength and modulus of elasticity reduction factors in current design codes are inadequate for steels utilized in the cold-formed steel construction industry [12-18].

This study conducted a numerical investigation utilizing Finite Element Method (FEM) software, LS-DYNA, to simulate failure conditions and to evaluate and propose various retrofit strategies. This research aimed to achieve two primary objectives: to analyze the failure mechanisms of the tensile fabric parking shed under wind-induced stress and to devise and assess practical retrofit solutions and design optimizations to mitigate future occurrences. Krzysztof Kosciuszko (2022) performed the study in Poland utilizing finite element method (FEM). The study's primary objective was to identify the factors contributing to the catastrophic destruction of the military tent. The simulation results accurately traced the failure development and identified the indications for implementing specific structural changes to the tent. The numerical calculations strongly correlated with actual observations and the model's behavior. Observations were conducted on the actual object, and the simulation results indicated that the tent, designed by applicable standards and utilizing less advanced computational tools (FEM in linear and nonlinear statics), may fail under the influence of impulsive wind. Advanced programs, such as LS-Dyna, are essential for calculations as they enable the model to account for factors including rapid and variable loads, large displacements, material nonlinearity, strain, and the velocity of structural destruction. An in-depth analysis of the probability of violent atmospheric phenomena, such as hurricanes, occurring at the expected location of the tent should precede the modeling. The canopy and its connection to the frame represent the tent's weakest link. These elements should be reinforced or constructed from plastic exhibiting greater tear strength [19]. Dayana Nima (2016) conducted a study to develop and validate a finite element model for roof assembly. The study utilized results from experimental cases to assess the static wind uplift force on flat roofs, employing both point load and distributed load assumptions. Additionally, the research aimed to apply the validated finite element model to update conservative FM design tables, considering allowable stresses and deflections [20].

Specifically, the objectives of this research are:

Spectrum of Engineering Sciences
SPECTRUM OF ENGINEERING SCIENCES
Online ISSN
3007-3138
Print ISSN
3007-312X

- To verify Numerical Models: Using LS-DYNA, create and verify a finite element model that faithfully replicates the dynamic wind load impact on parking shelters with arched roofs. This model will be compared to failure trends that have been noticed.
- To Provide Retrofit Solutions: Assess potential retrofits that might be used to improve the wind resistance of current parking structures. Enhancing material strength, connecting details, and overall structural arrangement will be the main goals of these solutions.
- To Optimize Design for New Structures: Based on the knowledge gathered from creative wind tunnel testing, make recommendations for design changes for new parking sheds. These suggestions aim to maximize new structures' structural stability and aerodynamic performance.

Methodology and Techniques

Site Investigation

Our research's site investigation phase was an attempt to precisely document the circumstances that led to the parking shed's collapse. It involved gathering much photographic evidence to record the collapse's aftermath. To aid in the creation of an intricate CAD model, we also took exact measurements of the remaining structure. We took the further step of getting material samples straight from the manufacturer to confirm the material qualities, even though the manufacturer said that A36 steel was used in the shed's construction. This ensured the accuracy of our later finite element modeling.

Uniaxial Testing of Sample Steel

To determine the exact mechanical characteristics of the material, we prepared specimens from the A36 steel sample that we had purchased from the shed's manufacturer to begin our uniaxial testing phase. Making dog bone specimens without a specialized specimen-cutting die was our first obstacle. The dog bone specimen failed too soon due to flaws created by the initial effort at local cutting with an angle grinder.

Spectrum of Engineering Sciences
SPECTRUM OF ENGINEERING SCIENCES
Online ISSN
3007-3138
Print ISSN
3007-312X

Figure 1: Locally Prepared Sample

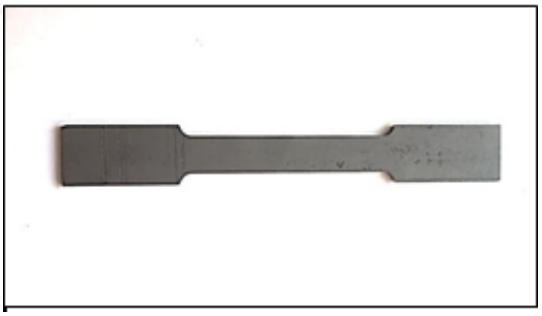

Figure 2: CNC Plasma Cut Sample

We solved this using the accuracy of CNC plasma cutting, guaranteeing millimeter-level precision in the specimens' shape. We created three specimens and tested their tensile strength using a universal testing machine (UTM). The displacement rate used in the testing procedure was UTM. The Stress Stain Curves were acquired.

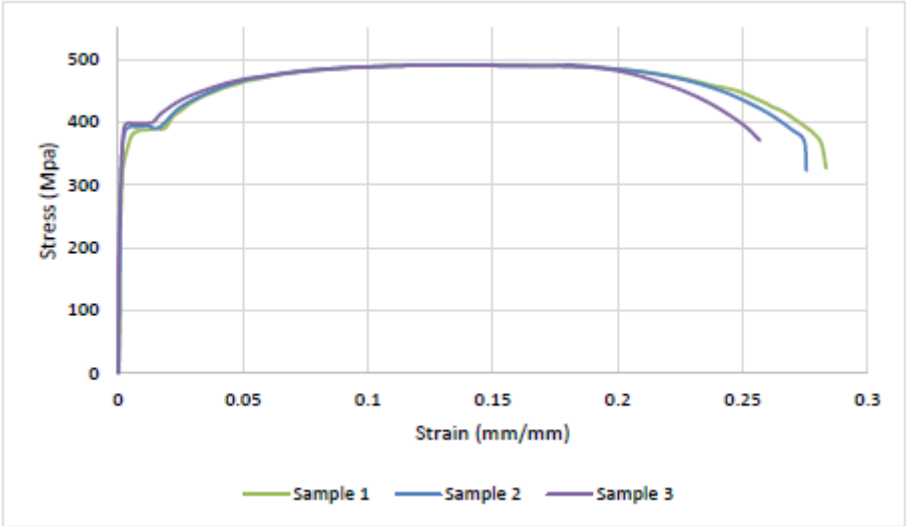

Figure 3: Stress-Strain Graph obtained from Uniaxial Testing

Table 1: Uniaxial Test Results in Tabulated Form

	Young's Modulus	Yield Strength	Tensile Strength
Sample 1	201 GPa	391.87 MPa	491.62
Sample 2	200 GPa	394.21 MPa	491.13
Sample 3	203 GPa	397.38 MPa	491.39
Average	201 GPa	394.48 MPa	491.38

For further FEA, we used the average results of the three samples.

Wind Load Calculation

Spectrum of Engineering Sciences
SPECTRUM OF ENGINEERING SCIENCES
Online ISSN
3007-3138
Print ISSN
3007-312X

Wind load calculations for a parking shelter are conducted according to the protocols outlined in ASCE 7-22. The aim is to comprehensively evaluate and improve the structure's resilience to heavy winds.

The shed was initially assigned a suitable risk category according to ASCE 7 criteria, which established the fundamental wind speed pertinent to the specific location, thereby considering regional climatic circumstances. The following phases included identifying essential characteristics for wind load computation, such as wind directionality factor, exposure category, topography factor, ground elevation factor, and gust-effect factors. The parameters were precisely calculated to accurately depict the wind forces operating on the structure and account for the impacts of internal and exterior pressures.

Table 2: Wind Load Calculations Steps

Step 1: Risk Category Determination	
Using Table 1.5-1	Risk Category 1
Step 2: Basic Wind Speed Determination	
From Building Code of Pakistan [5]	V=100 mph
Step 3: Wind Load Parameters	
Directionality Factor (k_d) from Table 26.6-1	K_d = 0.85 for arched roofs
Exposure Category from Section 26.7	Surface roughness B & Exposure Category B
Topographic factor, k_{zt} from section 26.8 and eq 26.8-1	K_{zt}= 1
Ground Elevation factor (k_e) for 1036 ft above sea level from Section 26.9	K_e = 0.96
Gust effect factor (G) for a Rigid structure from Section 26.11	G=0.85
Internal pressure coefficient (GC_{pi}) From Table 26.13-1	GC_{pi}=0 for open structures
Step 4: Determine velocity pressure exposure coefficient, Kz or Kh	
velocity pressure exposure coefficient, K_z or K_h from Table 26.10-1	K_z or K_h = 0.57

Spectrum of Engineering Sciences
SPECTRUM OF ENGINEERING SCIENCES
Online ISSN
3007-3138
Print ISSN
3007-312X

Step 5: Determine velocity pressure exposure coefficient, Kz or Kh	
Compute velocity pressure 'qz' or 'qh' from Equation(26.10-1)	'qz' or 'qh' = 11.62 psf Rounding off to 12 psf
Step 6: Determine external pressure coefficient, Cp or CN	
External pressure coefficient, Cp or CN from figure 27.3-3 for arched roofs based on rise to span ratio, r = 0.1045	Windward Cp = 0.146 psf Cen Cp = - 0.804 psf Leeward Cp = -0.5 psf
Step 7: Calculate wind pressure, 'p,' on each building surface	
Use Equation (27.3-2) for open buildings	Windward p = 1.26 psf Centre p = - 6.97 psf Leeward p = -4.335 psf

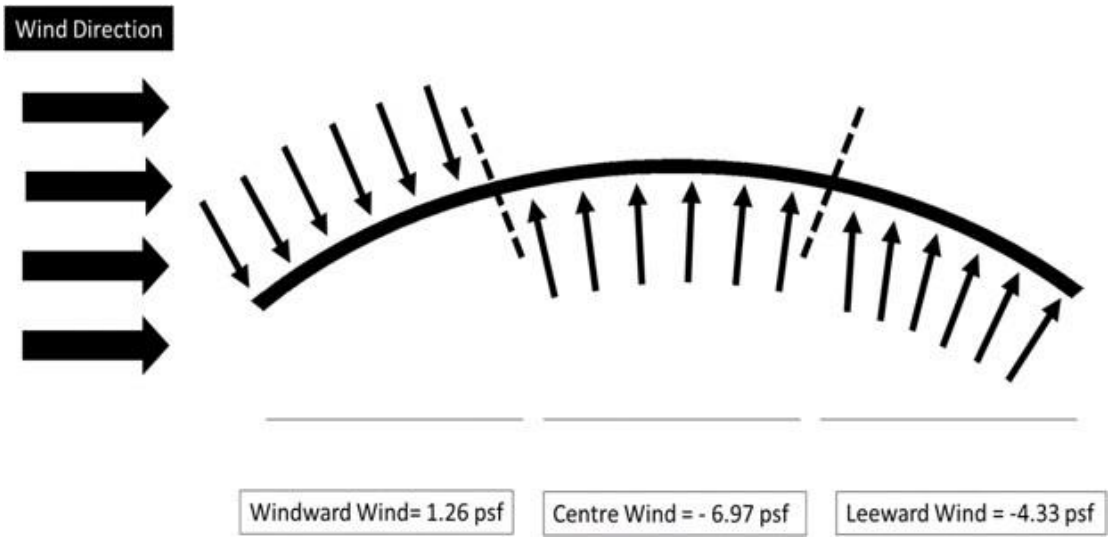

Figure 4: Wind Pressure Distribution on Arched Roof

LS DYNA - Finite Element Analysis

After the findings from the site investigation and load calculations, this study advanced to Finite Element Analysis (FEA), which initially required validating the material model. This was followed by benchmarking the shed's finite element model against empirical failure data. Each finite element model was constructed per the standards outlined in the LS-Dyna user manuals, employing LS-PrePost keycards.

Material Model Validation

This thesis's material model validation stage was essential to guarantee the precision of our finite element simulations in LS-DYNA.

Spectrum of Engineering Sciences
SPECTRUM OF ENGINEERING SCIENCES
Online ISSN
3007-3138
Print ISSN
3007-312X

To ensure the virtual representation accurately depicts the actual samples, we started by precisely CAD modeling the geometry of the dog bone specimens in the FEA environment. The specimen was modeled as shell elements to cut down on computing time. The model's meticulous meshing came next. A 2 mm mesh size was employed. An optimized mesh was essential to strike a compromise between computational efficiency and the level of detail required to portray the complex behavior of A36 steel.

Figure 5: CAD model of dog bone Specimen

Figure 6: Meshed Model

We adjusted the model parameters to match the empirical data obtained from uniaxial test data using the piecewise linear plasticity model (MAT 24), well-known for accurately portraying metals under stress.

Figure 7: Model showing Fixed and Displacement end

After that, one element in the failed region was probed to get the stress-strain curve seen in the figure.

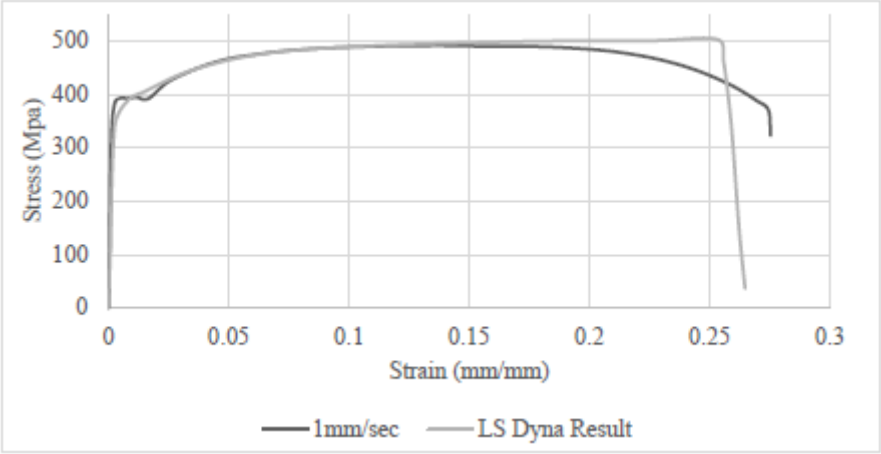

Figure 8: Stress-Strain Curve comparing LS Dyna results with actual test

The material model was verified because the LS Dyna findings

Spectrum of Engineering Sciences
SPECTRUM OF ENGINEERING SCIENCES
Online ISSN
3007-3138
Print ISSN
3007-312X

responded similarly to the uniaxial testing results. This validation procedure strengthened the validity of the material characteristics employed in the simulations, which are crucial in forecasting the parking shed's structural reaction under wind loading scenarios. It also strengthened the credibility of our ensuing structural studies.

Shed FE Model Benchmarking

An essential part of the thesis was the benchmarking phase for the parking shed's finite element model, which was created to compare the numerical model to the actual failure event. This procedure was necessary to confirm our LS-DYNA simulations' prediction precision and provide a solid basis for evaluating retrofit tactics.

The initial step in this phase was to recreate a precise CAD model of the parking shed using the LS PrePost program. The overhanging structure is modeled as 1D beam components to save time and computing effort, while the central column and cloth canopy are modeled as 2D shell elements.

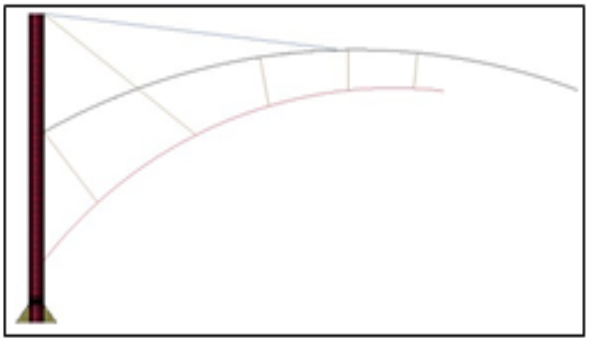

Figure 9: Side View of FE Model **Figure 10: Isometric View of FE Model**

A sophisticated meshing technique was used for the whole construction, striking a compromise between computing needs and the need for detail. To ensure the model correctly depicts the beginning and spread of failure, particular emphasis was given to regions vulnerable to stress concentrations. While the remaining components' mesh size was maintained

Vol. 2 No. 4 (2024)
Spectrum of Engineering Sciences
Online ISSN
3007-3138
Print ISSN
3007-312X
SPECTRUM OF ENGINEERING SCIENCES

significantly to save computing power, more accurate findings were achieved in more stress-induced places by utilizing a smaller mesh size for the primary column where the breakdown was seen.

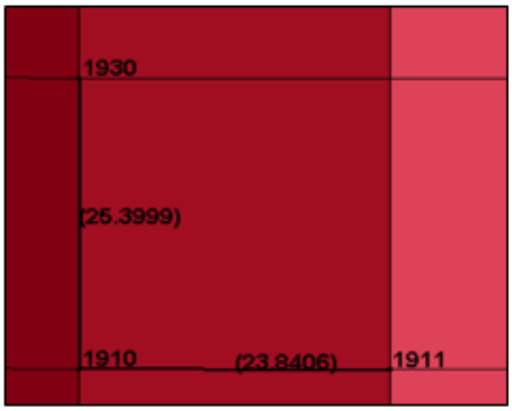

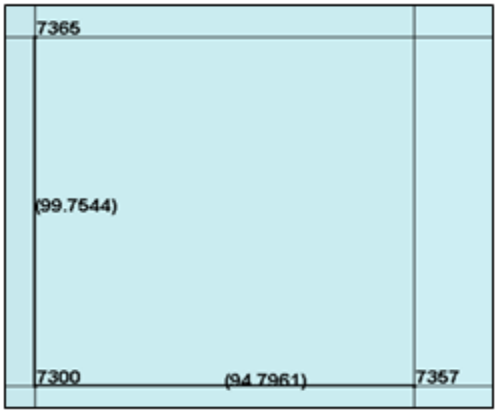

Figure 11: Finer Mesh in Main Column **Figure 12: Larger Mesh in Canopy**

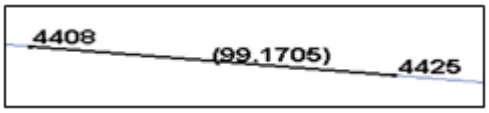

Figure 13: Larger Mesh in Overhang

MAT 24 specifications were used for the Steel structure in the simulation, using the verified material model from our previous uniaxial tensile testing. This application was essential because it made it possible for our analyses to precisely depict how the materials of the shed behaved under wind loads. On the other hand, the canopy was modeled as a rigid body using the MAT 20 Rigid material model to lower the computing power even though failure was not seen. Constraints and supports were added to the model to match the actual support requirements and simulate the boundary circumstances encountered by the parking shed. This feature was essential for guaranteeing that the wind loads given to the model would produce stress and deformation patterns that matched those seen following the shed's failure. All six degrees of freedom were fastened using a Boundary SPC keycard to secure the foundation plates.

Lastly, the model was subjected to the wind loads that had previously been established using the ASCE 7-22 criteria. Three sets of nodes were created based on the calculated wind loads. The load keycard was used to apply the pressure as the follower pressure of the canopy. This meant the force would stay perpendicular to the canopy even after the deformation began. To do this, we had to define a plane using three nodes in M1, M2, and

Spectrum of Engineering Sciences
SPECTRUM OF ENGINEERING SCIENCES
Online ISSN
3007-3138
Print ISSN
3007-312X

M3, and the force would act perpendicular to the plane's direction. This was done primarily to obtain accurate results. At the end of the benchmarking procedure, simulated findings resembled the failing shed's photographic proof. Furthermore, the stress-strain curve of the uniaxial test showed findings comparable to the yielding and failing values of the components at the failure region. Consequently, making sure the model has been compared to:

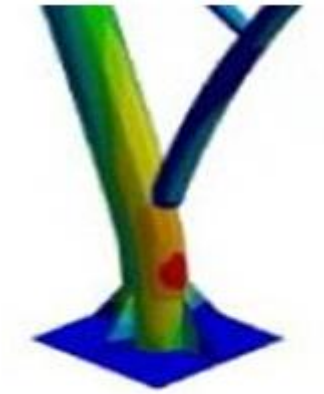

Figure 14: Failure in the FE model

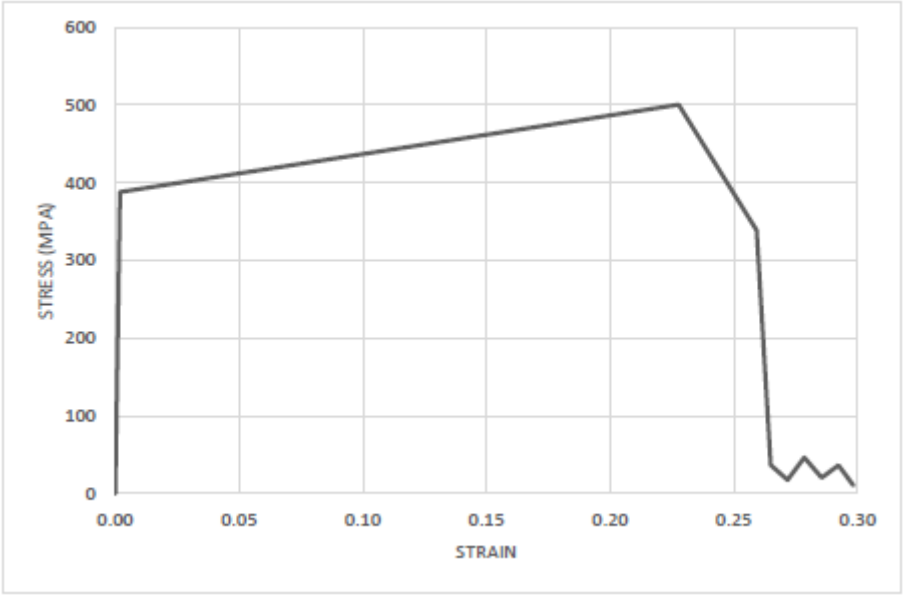

Figure 15: Stress-Strain Graph of Benchmarked Model in LS Dyna

In addition to validating our finite element model, this benchmarking revealed the shed's structural weaknesses, which helped us build retrofitting measures to prevent future occurrences of the same problems.

Strategies for Wind Load Effects Mitigation

Retrofit Suggestions using Benchmarked FE Model

The study, included in the section on retrofit recommendations for other

Spectrum of Engineering Sciences
SPECTRUM OF ENGINEERING SCIENCES
Online ISSN
3007-3138
Print ISSN
3007-312X

comparable existing buildings, involved two different retrofit designs integrated into the benchmarked finite element model. These changes increased the load-bearing capacity and structural resilience in high wind conditions.

First Retrofit Design: Addition of Support

The initial retrofit involved integrating a 3-inch diameter Hollow Structural Section (HSS) pipe as additional support at the shed's overhanging end. The results from the finite element analysis indicated that this retrofit was highly effective, as the stress levels in the model with the added support remained well below the critical threshold, peaking at 170 MPa. This stress level is significantly lower than the yield strength of 391 MPa, resulting in a favorable factor of safety (FOS) of 2.2, indicating robust structural performance.

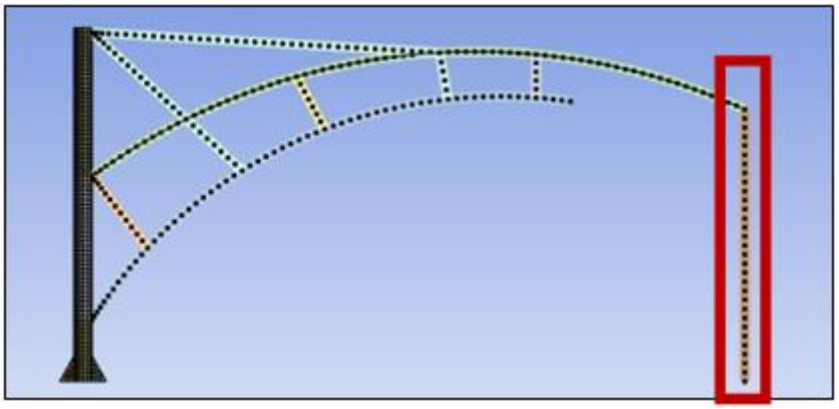

Figure 16: Supporting Column at Overhang End

Second Retrofit Design: Increasing Stiffeners Size

The stiffeners' height was increased from 177 mm to 300 mm as part of the second design change. The purpose of this modification was to improve the shed's structural integrity and stiffness, especially its capacity to sustain dynamic wind loads. With a maximum stress of 250 MPa, the finite element analysis for this updated model likewise produced encouraging findings. This stress value is larger than the previous retrofit model but is still less than the material's yield stress, resulting in a factor of safety (FOS) of 1.5. Though not as noticeable as the additional support retrofit, the larger stiffener size significantly improved the structural behavior under load.

Spectrum of Engineering Sciences
SPECTRUM OF ENGINEERING SCIENCES
Online ISSN
3007-3138
Print ISSN
3007-312X

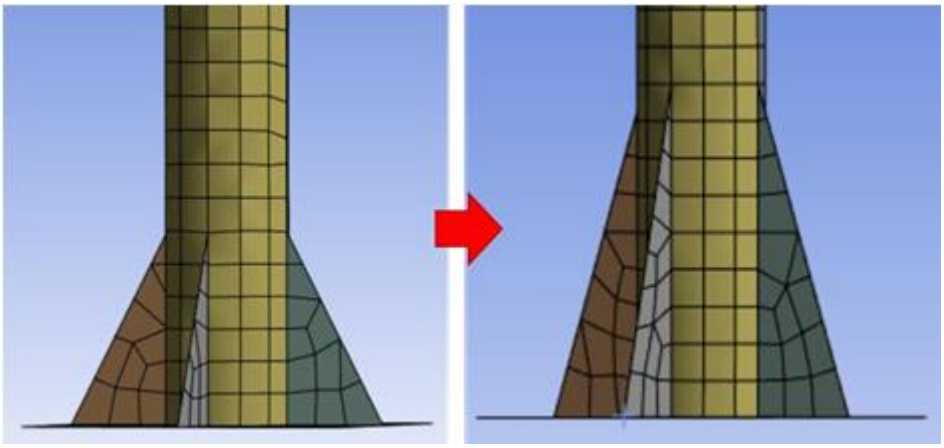

Figure 17: Increased Stiffeners Size

Comparative Analysis and Recommendations

It is clear from comparing the results of the two retrofit techniques in Figure 4.3 that both changes significantly increase the structural safety margins under unfavorable wind conditions. Adding a 3-inch HSS pipe support at the overhanging end was the best action regarding stress distribution and overall structural performance. To increase durability and resistance to strong winds, it is advised that comparable existing buildings take into account installing these retrofit designs, paying special attention to the extra pipe support.

This method guarantees these constructions fulfill and surpass the necessary safety requirements, offering a better safety factor and longer lifespan.

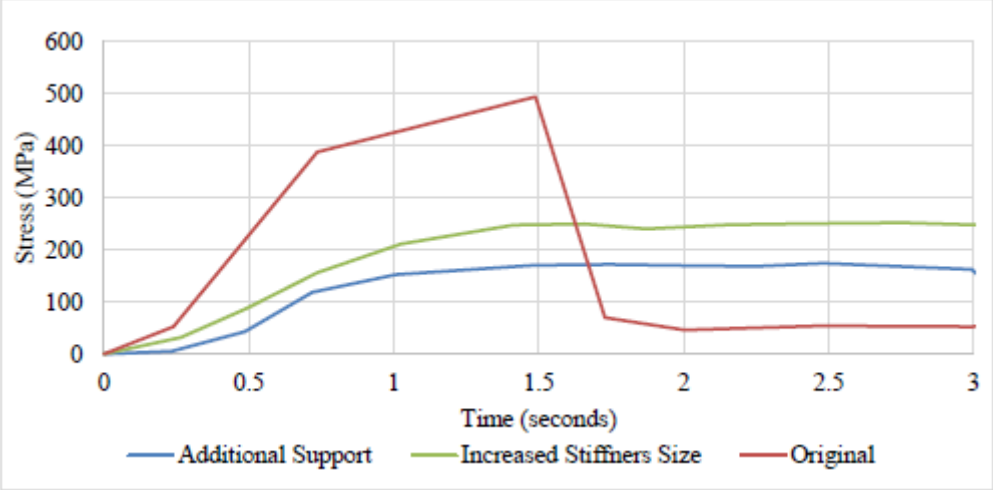

Figure 18: Stress Time Graph for Comparison

Canopy Design Optimization

The aerodynamic efficiency of three common canopy shapes, flat, gable, and arched, was thoroughly examined to optimize canopy design for new parking

Spectrum of Engineering Sciences
SPECTRUM OF ENGINEERING SCIENCES
Online ISSN
3007-3138
Print ISSN
3007-312X

shed constructions. To ensure precise proportions of functional parts necessary for aerodynamic testing, the research started with constructing an open-flow wind tunnel meticulously modeled in SketchUp.

Wind Tunnel Design and Construction

The wind tunnel was divided into four critical sections:

Contraction Zone: This section featured a design where air transitions from a larger to a smaller area at a 1:2 ratio, facilitated by a fan to generate the necessary airflow.

Airflow Straightener: Positioned after the contraction zone, this component aimed to minimize the formation of eddies, ensuring a smoother and more stable air flow conducive to precise measurements.

Test Section: Here, scaled models of the canopies were positioned for testing. This section was crucial for assessing the aerodynamic uplift forces exerted on different canopy designs under varied wind conditions.

Diffuser Section: This last section completed the airflow circuit by enabling the air to expand and exit the wind tunnel smoothly.

Once the virtual design was completed, the Sketch Up model's parameters built an actual wind tunnel. Furthermore, the option to modify the angle of attack was incorporated into the scaled models of the three canopy designs, enabling each model to be positioned from flat to slightly slanted. This adaptability was essential for evaluating how various wind orientations affected uplift.

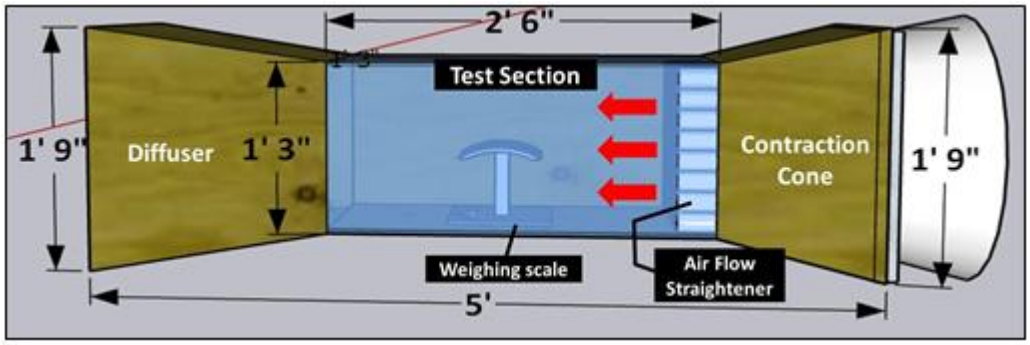

Figure 19: Labeled Sketch-Up Model of Wind Tunnel

Spectrum of Engineering Sciences
SPECTRUM OF ENGINEERING SCIENCES
Online ISSN
3007-3138
Print ISSN
3007-312X

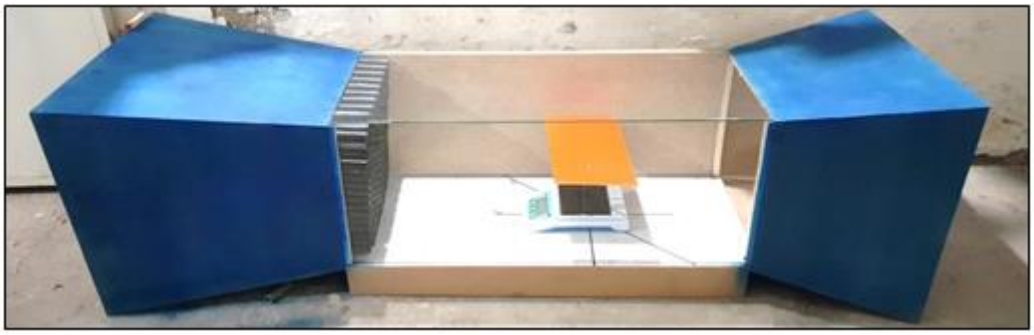

Figure 20: Actual Wind Tunnel

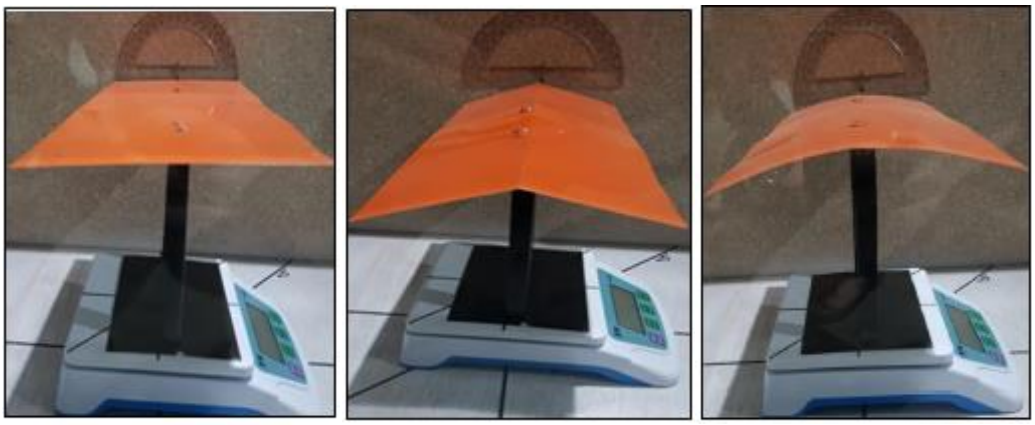

Figure 21: Flat Canopy Model, Gable Canopy Model, and Arched Canopy Model

Experimental Setup and Methodology

A precision weight scale with an accuracy of 0.1g was used inventively to quantify uplift forces. After setting each canopy model on the scale, it was tarred to zero. When the fan was turned on, the weight loss (opposing uplift force) was noted as the air pressure rose. Further testing altered the angle of attack from 0 to 15 degrees at 5-degree increments, allowing each design to be evaluated under wind directions of 0, 45, and 90 degrees.

Results and Analysis

According to the trial results, the flat canopy design was the most aerodynamically efficient configuration among the choices studied since it showed the least uplift. The gable canopy had the most significant uplift and, therefore, the least ideal aerodynamic qualities, while the arched canopy came in second with moderate rise.

Spectrum of Engineering Sciences
SPECTRUM OF ENGINEERING SCIENCES
Online ISSN
3007-3138
Print ISSN
3007-312X

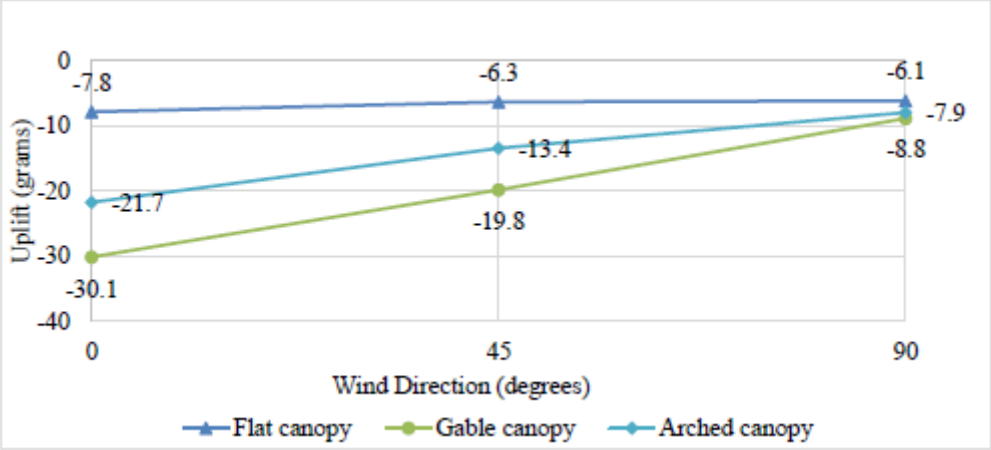

Figure 22: Uplift Measurements with Changing Wind Direction

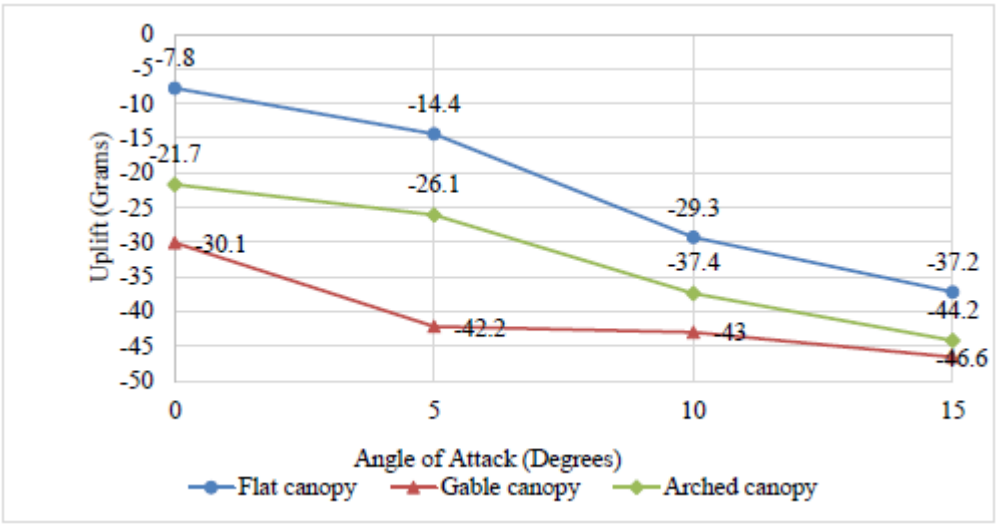

Figure 23: Uplift Measurements on Changing Angle of Attack with wind directionat 0 degrees

Spectrum of Engineering Sciences
SPECTRUM OF ENGINEERING SCIENCES
Online ISSN
3007-3138
Print ISSN
3007-312X

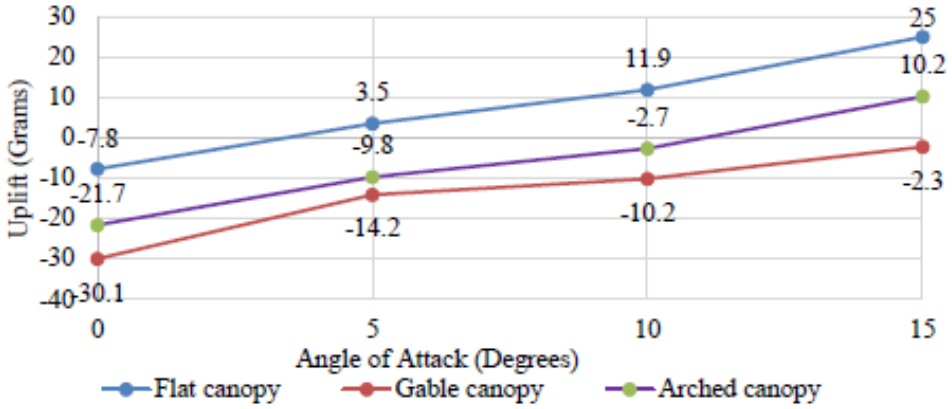

Figure 24: Uplift Measurements on Changing Angle of Attack with wind directionat 180 degrees

These results imply that the flat canopy design is the best option for reducing stress and improving the structural stability of parking shelters in new construction as it offers better resistance to wind-induced uplift.

Conclusions and Recommendations

Conclusions

Effective Simulation and Analysis

The parking shed's dynamic response to strong winds was successfully captured by using LS-DYNA finite element analysis with wind loads determined by ASCE 7-22 Minimum Design Loads and Associated Criteria for Buildings and Other Structures (2021). This method offered essential insights into the structural weaknesses by faithfully simulating the circumstances that caused the building to fail.

Critical Structural Vulnerabilities Identified

The analysis identified significant structural flaws, especially in the parking shed's central column, which prompted us to devise retrofitting measures that included strengthening the overhanging ends and enlarging the stiffeners. These measures were crucial in causing the structure to collapse during the windstorm.

Successful Retrofit Strategies

The tested and designed retrofit techniques greatly increased structural resilience, including enlarging the stiffeners and adding a 3-inch HSS pipe at the overhanging ends. According to the FEA results, these changes successfully decreased stress levels, improving structural safety against loads brought on by wind.

Spectrum of Engineering Sciences
SPECTRUM OF ENGINEERING SCIENCES
Online ISSN
3007-3138
Print ISSN
3007-312X

Canopy Design Optimization Proven Effective

An inventive method for measuring uplift in a specially constructed wind tunnel was using a high-precision weighing scale. This method yielded precise and trustworthy data on uplift for various canopy designs, ultimately demonstrating that the flat canopy design performed best in terms of reducing aerodynamic uplift. This result is essential for the construction of new structures where aerodynamic efficiency is critical.

Recommendations

Implementation of Retrofit Solutions

Existing structures akin to the examined parking shed are advised to implement the verified retrofit options to improve their wind resistance. The incorporation of the 3-inch HSS pipe support should be prioritized because of its substantial efficacy in significantly alleviating stress levels.

Guidance for New Constructions

For new parking shed structures, a flat canopy design is recommended since it has demonstrated superior efficacy in mitigating wind uplift. Design criteria must be revised to incorporate this preference for optimizing aerodynamic efficiency and structural integrity.

Further Research on Material and Design Variations

Further investigation into various materials and design alterations is recommended to improve the durability and safety of tensile fabric structures. Investigating innovative materials with enhanced tensile strength and flexibility may yield novel methods to improve structural performance under harsh situations.

By addressing these results and executing the proposed changes, the robustness of tensile fabric structures to wind loads may be markedly enhanced, resulting in safer and more dependable infrastructure.

Acknowledgment

We thank our senior academic members and lab administrators for their unwavering support and guidance during this project. Their expertise, assistance, and provision of supplies were essential to completing this job. This article is dedicated to them for their invaluable contributions.

References

1. Di Lorenzo, G., Formisano, A., Terracciano, G., & Landolfo, R. (2021). Iron alloys and structural steels from XIX century until today: Evolution of

Spectrum of Engineering Sciences
SPECTRUM OF ENGINEERING SCIENCES
Online ISSN
3007-3138
Print ISSN
3007-312X

mechanical properties and proposal of a rapid identification method. Construction and building materials, 302, 124132.

2. Guo, T., & Chen, Y. W. (2011). Field stress/displacement monitoring and fatigue reliability assessment of retrofitted steel bridge details. Engineering Failure Analysis, 18(1), 354-363.

3. Kühn, B., Lukic, M., Nussbaumer, A., Günther, H. P., Helmerich, R., Herion, S. H. K. M., ... & JRC, E. (2008). Assessment of existing steel structures: recommendations for estimation of remaining fatigue life.

4. Schroot, D. (2016). Performance of retrofitted steel structures subjected to fatigue loading. In Insights and Innovations in Structural Engineering, Mechanics and Computation (pp. 1954-1959). CRC Press.

5. Chan, T. H., Guo, L., & Li, Z. X. (2003). Finite element modelling for fatigue stress analysis of large suspension bridges. Journal of Sound and Vibration, 261(3), 443-464.

6. Leon, R. T., & Gao, Y. (2016). Resiliency of steel and composite structures. Frontiers of Structural and Civil Engineering, 10, 239-253.

7. Kiakojouri, F., De Biagi, V., Chiaia, B., & Sheidaii, M. R. (2022). Strengthening and retrofitting techniques to mitigate progressive collapse: A critical review and future research agenda. Engineering structures, 262, 114274.

8. Solari, G. (2017, November). Wind loading of structures: Framework, phenomena, tools and codification. In Structures (Vol. 12, pp. 265-285). Elsevier.

9. Standard, B. (1990). Structural use of steelwork in building, Part 8: Code of practice for fire resistant design. British Standard Institution.

10. Buchanan, A. H., & Abu, A. K. (2017). Structural design for fire safety. John Wiley & Sons.

11. Sidey, M. P., & Teague, D. P. (1988). Elevated temperature data for structural grades of Galvanised steel. British Steel (Welsh Laboratories) Report.

12. Ranawaka, T., & Mahendran, M. (2009). Experimental study of the mechanical properties of light gauge cold-formed steels at elevated temperatures. Fire safety journal, 44(2), 219-229.

13. Kankanamge, N. D., & Mahendran, M. (2011). Mechanical properties of cold-formed steels at elevated temperatures. Thin-Walled Structures, 49(1), 26-44.

Spectrum of Engineering Sciences
SPECTRUM OF ENGINEERING SCIENCES
Online ISSN
3007-3138
Print ISSN
3007-312X

14. Mäkeläinen, P., Outinen, J., & Kesti, J. (1998). Fire design model for structural steel S420M based upon transient-state tensile test results. Journal of constructional steel research, 48(1), 47-57.
15. Chen, J., & Young, B. (2007). Experimental investigation of cold-formed steel material at elevated temperatures. Thin-Walled Structures, 45(1), 96-110.
16. Chen, J., & Young, B. (2006). Corner properties of cold-formed steel sections at elevated temperatures. Thin-Walled Structures, 44(2), 216-223.
17. E. Mecozzi, B. Zhao, Development of stress-strain relationships of cold-formed lightweight steel at elevated.
18. Outinen, J., & Mäkeläinen, P. (2004). Mechanical properties of structural steel at elevated temperatures and after cooling down. Fire and materials, 28(2-4), 237-251.
19. K. Kosiuczenko, "Numerical investigation of hurricane-induced failure of a military tent," 2022. [Online]. Available: https://www.researchgate.net/publication/375331715
20. Nima Dayani, "Numerical and Experimental Investigations for Wind Uplift Force on Flat Roofing System," University of Ottawa, 2016.

List of Symbols, Abbreviations and Acronyms

FEM	Finite Element Modelling
FE	Finite Element
FEA	Finite Element Analysis
ASCE	American Society of Civil Engineers
NIT	National Institute of Transportation
ASTM	American Society for Testing & Materials
LSTC	Livermore Software Technology Corporation
HSS	Hollow structural section